Environmental Science & Technology

pubs.acs.org/est

Article

Changing Nature of Organic Carbon over the United States

Amy E. Christiansen,* Annmarie G. Carlton, and William C. Porter

Cite This: *Environ. Sci. Technol.* 2020, 54, 10524−10532

Read Online

ACCESS | Metrics & More | Article Recommendations | Supporting Information

ABSTRACT: Total organic carbon (TOC) mass concentrations are decreasing across the contiguous United States (CONUS). We investigate decadal trends in organic carbon (OC) thermal fractions [OC1 (volatilizes at 140 °C), OC2 (280 °C), OC3 (480 °C), OC4 (580 °C)] and pyrolyzed carbon (PC), reported at 121 locations in the *I*nteragency *M*onitoring of *Pro*tected *V*isual *E*nvironments (IMPROVE) network from 2005 to 2015 for 23 regions across the CONUS. Reductions in PC and OC2 drive decreases in TOC (TOC = OC1 + OC2 + OC3 + OC4 + PC) mass concentrations. OC2 decreases by 40% from 2005 to 2015, and PC decreases by 34%. The largest absolute mass decreases occur in the eastern United States, and relative changes normalized to local concentrations are more uniform across the CONUS. OC is converted to organic mass (OM) using region- and season-specific OM:OC ratios. Simulations with GEOS-Chem reproduce OM trends and suggest that decreases across the CONUS are due to aerosol liquid water (ALW) chemistry. Individual model species, notably aerosol derived from isoprene oxidation products and formed in ALW, correlate significantly ($p < 0.05$) with OM2, even in arid regions. These findings contribute to literature that suggests air quality rules aimed at SO_2 and NO_x emissions induce the cobenefit of reducing organic particle mass through ALW chemistry, and these benefits extend beyond the eastern United States.

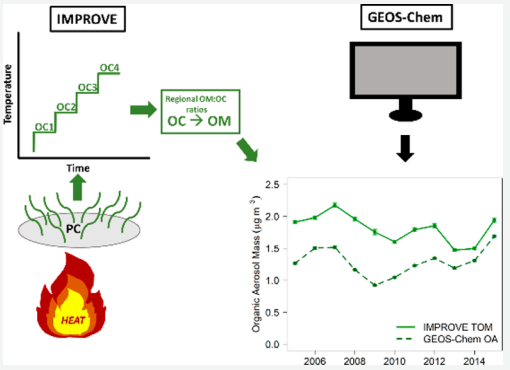

1. INTRODUCTION

Concentrations of organic carbon (OC), a major contributor to fine particulate matter ($PM_{2.5}$) mass,[1] have decreased over past decades across the contiguous United States (CONUS), notably in the southeastern United States.[2−6] Carbon-14 analysis at rural locations such as national parks revealed that most OC is nonfossil in these areas and presumably derived from biogenic emissions,[7,8] which are projected to increase as the climate warms.[9] In urban and near-urban locations, residential heating and cooking contributes some amount of nonfossil carbon-14, but this is not a significant contributor at remote locations.[8,10] Smoke from wildfires, which are increasing in frequency, intensity, and acreage burned,[11,12] also contribute nonfossil carbon to the total organic carbon (TOC). Decreases in OC are attributable to the effects of anthropogenic NO_x and SO_2 regulations,[13] the impetus of which was to reduce acid deposition in the eastern United States and ozone mixing ratios. This reduces surface mass concentrations of sulfate and nitrate,[2] hygroscopic PM constituents that facilitate aerosol liquid water (ALW) formation and secondary organic aerosol (SOA), in turn reducing contributions to OC in observations in the southeastern United States[3] and in model simulations of the CONUS.[13,14] The Community Multiscale Air Quality (CMAQ) and GEOS-Chem models better reproduce observed decadal trends most successfully when the SOA chemical mechanism includes water-mediated chemistry and uptake, in particular in the eastern United States.[15]

The *I*nteragency *M*onitoring of *Pro*tected *V*isual *E*nvironments (IMPROVE) network provides the longest continuous measurements of surface ambient concentrations of carbonaceous material in $PM_{2.5}$ across the United States using thermal optical organic carbon/elemental carbon (OC/EC) analyzers.[16,17] Organic and elemental carbon mass concentrations are measured from the evolution of organic species from a filter at operationally defined temperatures. Mass measurements of OC are made by heating filters in a helium environment to allow organic species to volatilize without oxidation on the filter. Organic species tend to pyrolyze above 300 °C,[18] and this pyrolysis is monitored and corrected via reflectance.[19] The IMPROVE network defines four OC thermal fractions (OC1, OC2, OC3, and OC4) at temperatures ranging from 140 to 580 °C,[20] a protocol applied routinely since 2005, to minimize the amount of OC that undergoes pyrolysis during analysis.[19−21] OC fraction measurements provide information about the volatility of the organic species within each fraction

Received: April 9, 2020
Revised: May 22, 2020
Accepted: May 28, 2020
Published: May 28, 2020

https://dx.doi.org/10.1021/acs.est.0c02225
Environ. Sci. Technol. 2020, 54, 10524−10532

and not specific chemical identity. There are a number of uncertainties within these fractions, including pyrolysis, interactions from other species,[22−24] and analytical biases.[25] However, previous studies have used OC fractions to provide chemical insight regarding speciation and sources.[26−29] Field campaigns in locations around the world, using a previous iteration of the IMPROVE thermal protocol, identify biomass burning and anthropogenic combustion processes as major sources of OC1 and OC2[26−28] and cooking emissions and dust as sources that contribute to OC3 and OC4.[26,29] A laboratory analysis of individual organic compounds found widely in the atmosphere (e.g., oxalic acid, levoglucosan, azelaic acid, and humic-like substances) discovered that as the molecular weight of an organic species increases, higher temperatures are needed for carbon evolution.[30] Efforts to identify specific organic functional groups[31−33] and other chemical properties, including viscosity,[34] from filters analyzed for TOC content are an active area of research.

Changing chemical regimes for ozone in response to decreases in anthropogenic NO_x emissions in the atmosphere of the CONUS are noted in the literature.[35] This changing photochemistry may also affect SOA formation pathways in ways that affect the overall nature of particulate organic carbon by altering speciation, degree of oxidation, and phase state. Volatile organic carbon (VOC) reacts with various oxidants and forms peroxy radicals (RO_2) in the presence of oxygen.[36] Traditionally, the fate of an RO_2 species is assumed to be predominantly driven by its bimolecular reaction with NO, HO_2, or another RO_2. However, as NO_x emissions decrease, autoxidation reactions become more important, potentially leading to more highly oxidized organic species.[37] Decadal changes in OC fraction mass concentrations and relative fractional contribution to the total may indicate changes in SOA speciation, oxidation, and other properties. In 2019, Hand et al.[38] cautiously suggested that organic aerosol (OA) across the CONUS is increasingly aged and oxidized over time, although analytical bias in the separation of OC and EC confound interpretation.[25]

Previous studies of temporal trends in OA and particulate OC focus on TOC measurements,[2−4] and decadal trends in the individual thermal fractions have not received as much analysis in the literature. Here, we investigate geospatial and temporal trends in OC fractions to determine which contribute significantly to overall TOC decreases. We also track decadal changes in OA from 2005 to 2015 in the GEOS-Chem model to identify potential OC sources and formation mechanisms that may help to explain observed trends.

2. MATERIALS AND METHODS

2.1. Surface Measurements and Estimates. IMPROVE network chemical speciation data were downloaded from http://vista.cira.colostate.edu/Improve/ on February 26, 2020, for 121 sites across the CONUS with >80% of sampling days reported from 2005 to 2015 [Figure S1a, Supporting Information (SI)]. These years correspond to a change in the thermal protocol in 2005[20] and a change in the instrument after 2015.[39] We use all reported values and uncertainties. Values below the method detection limit (MDL) are kept in the analysis when the value plus uncertainty is above the MDL. Uncertainties are reported as measures of standard deviation,[40] and there is an equal chance that these values fall above or below the MDL. Since these values may exceed the MDL, we keep them in our analysis. Rural sites are grouped into 23 chemical climatology regions defined by IMPROVE as having similar aerosol composition and topography (Figure S1b, SI),[6] and each region in our analysis contains between 2 and 10 sites. We use surface mass concentration data of thermally defined OC fractions OC1 (140 °C), OC2 (280 °C), OC3 (480 °C), and OC4 (580 °C), PC, and TOC (OC1 + OC2 + OC3 + OC4 + PC) across these chemical climatology regions. OC1 concentrations are assumed to be a lower bound due to volatilization of species during field latency, transport, and storage.[41] We report OC1 trends and concentrations since they are reported by the IMPROVE network, but we do not attempt to assign chemical meaning due to high levels of uncertainty. OC4 is the least volatile fraction.

The OC fractions are operationally defined, and there is debate about how method differences impact quantification of OC and EC.[23] IMPROVE uses one of several thermal/optical reflectance analysis protocols, and we limit our analysis to this method to avoid intercomparison issues. Some analytical biases may still persist.[22−24,41,42] Semivolatile species, such as ammonium nitrate[43] and OC1, are lost from filter samples before and during analysis.[41,42] Metal salt particles, particularly ones containing copper and iron, can reduce the oxidation temperature of EC and enhance OC charring, affecting the OC/EC split and reported TOC concentrations.[22] KCl and NaCl from biomass smoke and sea spray can also alter the temperature at which large organic compounds and EC evolve.[23] CONUS-averaged copper and iron concentrations do not appreciably change, and sea salt concentrations do not trend positive or negative from 2005 to 2015 (Figure S2, SI). Further, we use median values in our analysis to minimize the impact of episodic outliers, such as wildfires and biomass burning. Water-soluble organic carbon (WSOC) characteristic of rural aerosol is susceptible to pyrolysis during analysis.[16] Total pyrolyzed carbon (PC) is measured in a separate category from the thermal fractions and cannot be assigned to a particular step in the temperature ramp. Hence, reported mass concentrations for OC fractions are lower mass bounds because some of each fraction may be lost to charring and counted as PC.[16] Recently, Malm et al. (2020)[25] demonstrated that PC and EC coevolve, causing lower-temperature oxidation of EC,[44,45] which biases TOC concentrations high because it includes some EC. It is difficult to quantitatively assess how PC impacts individual OC fraction trends. While there are uncertainties and precautions to take when using OC fraction data, the IMPROVE record is the oldest continuous TOC network in the CONUS, and the underutilized OC fraction data may facilitate insight regarding the controlling mechanisms responsible for the decrease in TOC and its changing nature.

The IMPROVE protocol measures particulate organic carbon, yet organic aerosol is composed of other elements, such as hydrogen, oxygen, nitrogen, and sulfur, that are not accounted for in these measurements. Often, an OM:OC ratio of 1.8 is applied as a factor to account for noncarbon organic mass, though ratios vary spatially, seasonally, and decadally and depend on air mass origin.[38,46−49] Several methods of OM:OC ratio determination are discussed in the literature. In 2005, El-Zanan et al.[48] experimentally determined OM:OC ratios at five IMPROVE sites representative of their chemical climatology regions using subsequent solvent extractions of dichloromethane, acetone, and water. Other methods include multiple linear regression approaches based on reported IMPROVE measurements,[46] a combination of aerosol mass spectrometers

https://dx.doi.org/10.1021/acs.est.0c02225
Environ. Sci. Technol. 2020, 54, 10524−10532

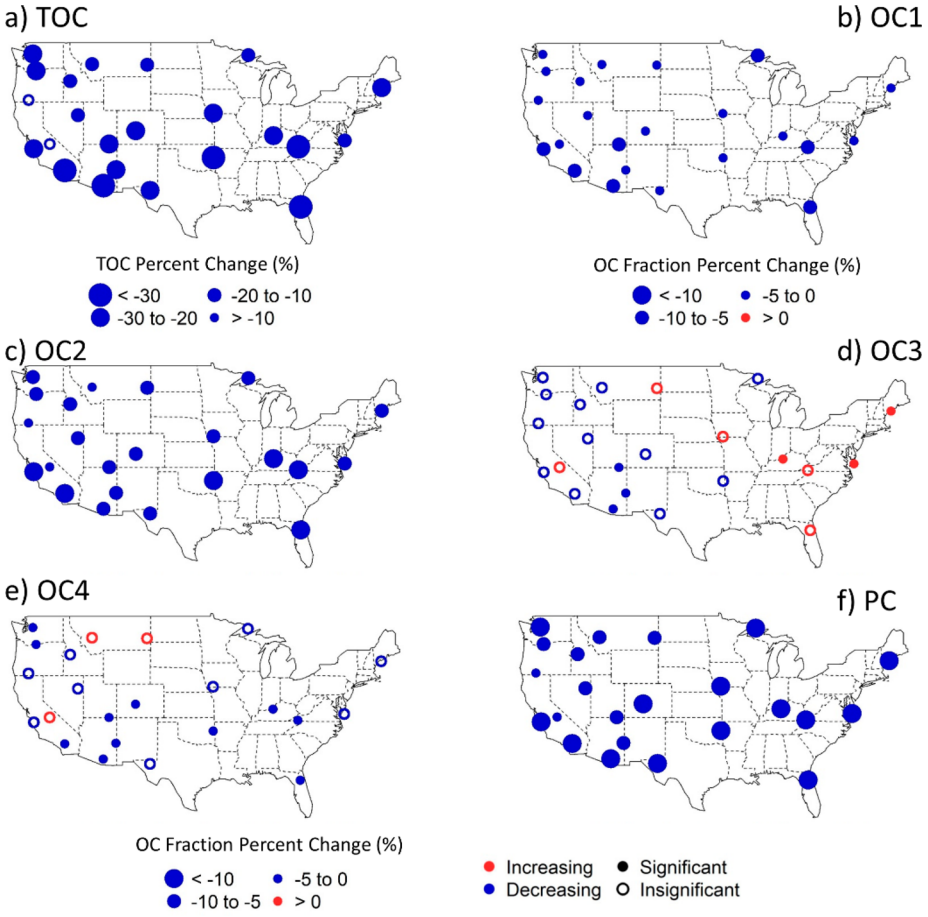

Figure 1. Maps of relative decadal trends (2005−2015) in (a) TOC, (b) OC1, (c) OC2, (d) OC3, (e) OC4, and (f) PC mass concentrations for each chemical climatology region. Size corresponds to the magnitude of the percent change. Red indicates an increasing trend, blue indicates a decreasing one, a colored circle indicates that the increase or decrease is significant ($p < 0.05$) by the Mann−Kendall test, and an unfilled circle indicates that the change is insignificant.

(AMS) and satellite NO_2 data,[47] and functional group information derived from Fourier-transform infrared (FT-IR) spectra of IMPROVE samples.[50] Across all analyses, OM:OC ratios ranged from 1.3 to 2.6. Ratios are highest in the summer and rural areas and lowest in the winter and urban areas.[46,47] Average OM:OC ratios across the CONUS may be increasing with time (Figure S3, SI),[38] although analytical biases that apportion some light-absorbing carbon (LAC) to OC[25] cannot be ruled out.

We determine seasonal organic mass (OM) for all regions across the CONUS with >80% complete data from 2005 to 2015 using OM:OC ratios determined via mass balance using IMPROVE-defined reconstructed mass[51] and removing the 1.8 multiplier from OC (eq 1) as summarized by Malm et al. in 2020.[25,48,52] OM:OC ratios using this method are subject to the same biases as filter measurements detailed above, such as the loss of semivolatile species.[22−24,41,42,53]

$$\text{OM: OC} = \frac{PM_{2.5} - (NH_4)_2SO_4 - NH_4NO_3 - EC - SOIL - 1.8 \times Cl}{OC} \quad (1)$$

Here, SOIL is equal to $(2.2 \times Al + 2.49 \times Si + 1.63 \times Ca + 2.42 \times Fe + 1.94 \times Ti)$.[51] We convert IMPROVE-measured OC to OM estimates for a more direct comparison to GEOS-Chem simulations because the model provides OA mass concentrations. Each OC fraction and TOC is multiplied by the appropriate seasonal and regional OM:OC ratio, and they are referred to as OM fractions and TOM.

ALW mass concentrations are estimated using the thermodynamic equilibrium model ISORROPIA version 2.1, publicly available online.[54] Temperature and relative humidity (RH) data were extracted from the North American Regional Reanalysis (NARR) model as in the work of Nguyen et al.[55]

Three-hour temperature and RH data are averaged to 24 h to match the 24-h sampling time of IMPROVE measurements. ALW concentrations are estimated at each available IMPROVE sampling day. We assume metastable conditions and use only SO_4^{2-} and NO_3^- mass concentrations since NH_4^+, which increases ALW, is not measured at IMPROVE sites. We do not include dust and organic species due to large water uptake uncertainties[56−58] and the spatial heterogeneity in dust, which would disproportionately affect uncertainties in ALW estimations across regions. Our approach affects absolute values of ALW, but it does not affect overall interpretation or broad trends, consistent with previous analyses that use the

https://dx.doi.org/10.1021/acs.est.0c02225
Environ. Sci. Technol. 2020, 54, 10524−10532

same method and include organic compounds[3] and dust[59] in sensitivities of ALW estimates.

2.2. GEOS-Chem Modeling. Observations are paired in space and time via a nearest-neighbor approach with model predictions from GEOS-Chem version 12.3.2 (http://acmg.seas.harvard.edu/geos) driven by the MERRA-2 reanalysis product[60] developed by the NASA Global Modeling and Assimilation Office (GMAO). Nested 0.5° × 0.625° simulations over North America are examined across 2005−2015 using output from global simulations run at 2° × 2.5° horizontal resolution to provide boundary conditions. Anthropogenic emissions for the United States are taken from the National Emissions Inventory 2011 (NEI11) developed by the United States Environmental Protection Agency (EPA), as implemented in GEOS-Chem by Travis et al.[61] and adjusted for trends over time using the EPA's national annual scaling factors. Online biogenic emissions are provided by the Model of Emissions of Gases and Aerosols from Nature (MEGAN)[62] with updates for acetaldehyde emissions[63] and CO_2 dependence.[64] Biogenic emissions vary over time on the basis of ambient meteorological conditions, as do trends in leaf area index (LAI), which are captured using the MODIS-derived LAI data product from Yuan et al.[65] Fire emissions are modeled using the fourth-generation Global Fire Emissions Database (GFED4).[66,67] Inorganic aerosol thermodynamics are modeled using the ISORROPIA 2.2 module,[54] while SOA formation is represented by the simplified Volatility Basis Set (VBS) approach of Pye et al.[68] with the addition of the nonreversible aqueous-phase isoprene SOA scheme of Marais et al.[15] We include 13 speciation bins in our analysis (defined in Table S1, SI). Note that we treat the bins INDIOL (organonitrate hydrolysis products) and ISOAAQ (aerosol from the aqueous isoprene mechanism) separately. While INDIOL includes contributions from gas-phase isoprene oxidation products, lifetimes are uncertain[69] and INDIOL is by default excluded from mass summation calculations in GEOS-Chem.

We determine the direction and significance of relative decadal trends in particulate OC, OC converted to OM, and predicted GEOS-Chem speciation bins (Table S1, SI) using Sen's slope and the Mann−Kendall test, nonparametric techniques that are resistant to outliers and account for seasonality, in R statistical software.[70−74] We define winter as December, January, and February (DJF), spring as March, April, and May (MAM), summer as June, July, and August (JJA), and fall as September, October, and November (SON).

3. RESULTS AND DISCUSSION

Across the CONUS, absolute and relative OC1, OC2, and PC mass concentrations exhibit statistically significant ($p < 0.05$) decreasing trends over time in all chemical climatology regions [Figures 1 and S4 (SI)], as does the TOC with the exception of two regions in California. The median TOC concentration across the CONUS decreases from 0.78 $\mu g\ m^{-3}$ in 2005 to 0.64 $\mu g\ m^{-3}$ in 2015. OC2 and PC drive TOC mass concentration decreases. Species in OC2 may contain carboxylic acids, polyaromatic hydrocarbons (PAHs), and steranes.[17] PAHs and steranes are anthropogenic emissions markers for incomplete fossil fuel combustion and motor oil emissions,[75−77] and carboxylic acids originate from oxidation of biogenic and anthropogenic VOCs or direct emission from fossil fuel combustion and biomass burning.[78] Changes in PC may be due to misapportioned EC,[25] and some laboratory analyses connect PC to WSOC.[16] OC2 and PC decreases are ubiquitous and significant ($p < 0.05$), with the largest absolute and relative decreases occurring in the eastern United States, where ALW mass concentrations and relative decreases in ALW are also the greatest (Figures S4−S6, SI).[55,79] These decreases are generally larger than measurement uncertainties, especially in the southeastern United States (Figure S7, SI). OC3 increases in three chemical climatology regions in the humid eastern United States over the same time period, especially during summer (Figure S8, SI) after 2013 (Figure 2).

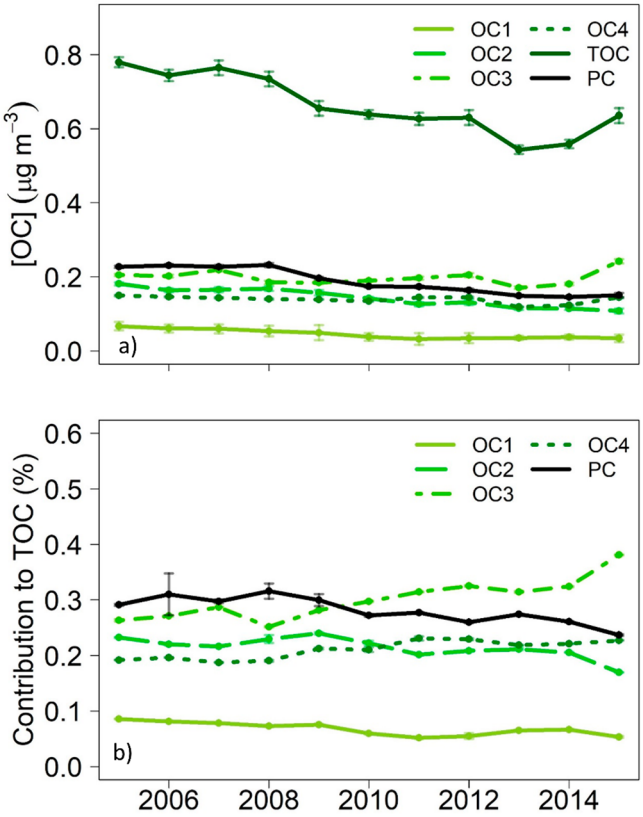

Figure 2. Decadal trends across the CONUS for (a) the TOC, OC fraction, and PC mass concentrations and (b) fractional contribution of OC fractions and PC to the TOC. Error bars represent the standard error of the medians.

The magnitude of decadal changes among the OC fractions varies within and across regions, and OC fractional contributions to the TOC differ from 2005 to 2015 (Figure 2). OC2 mass concentrations decrease significantly ($p < 0.05$) by a total of 0.07 $\mu g\ m^{-3}$, from 23% of the TOC to 17%. By contrast, OC3 mass concentrations across the CONUS increase by 0.03 $\mu g\ m^{-3}$, from 27% of the TOC to 38%, and contribute the most by mass to the CONUS-averaged TOC after 2010. Over the decade from 2005 to 2015, these increases are significant in three regions in the eastern United States. OC4 mass concentrations decrease by less than 0.01 $\mu g\ m^{-3}$; however, the fractional contribution of OC4 to the TOC increases from 19% to 23%. Median publicly reported OC1 mass concentrations decrease by more than 50%. In 2005, across the CONUS, PC concentrations are higher than any OC fraction at 0.23 $\mu g\ m^{-3}$ and decrease to 0.15 $\mu g\ m^{-3}$ by 2015 (29% of the TOC to 24%). The rate of decline for PC is

https://dx.doi.org/10.1021/acs.est.0c02225
Environ. Sci. Technol. 2020, 54, 10524−10532

significant, higher than that for any OC fraction, and is spatially consistent with the largest decreases in ALW (Figures S5 and S6, SI). Decadal declines in OC2 are statistically robust and larger than measurement uncertainties, and OC2 is less likely to pyrolyze than fractions evolving at higher temperatures.[18]

GEOS-Chem reproduces spatial and temporal trends in IMPROVE-estimated total organic mass (TOM) using region- and season-specific OM:OC ratios across the CONUS (Figure 3). Individual GEOS-Chem simulated organic aerosol

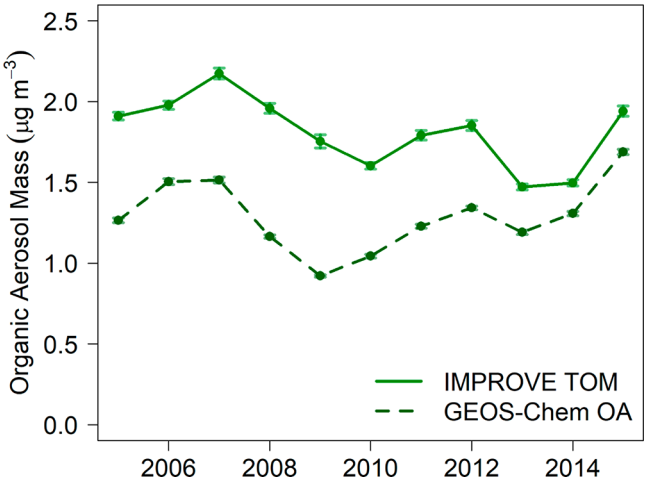

Figure 3. IMPROVE TOM and GEOS-Chem predictions of the TOA across the CONUS from 2005 to 2015. Standard errors are represented via error bars.

speciation bin mass concentrations correlate significantly ($p < 0.05$) with specific IMPROVE OM fractions in every region and season, offering plausible mechanistic insight into these changes. Significant correlations ($p < 0.05$) between predicted OA and estimated OM fractions are found in each region and indicate that some chemical complexity tied to formation pathways is captured by OC fraction measurements in routine network data. Over all regions and seasons, we assess 13 model species (Table S1, SI) and compare them with OM fractions. We find 739 significant paired evaluations over 11 years in 23 regions. Correlations are positive and occur frequently among water-mediated species and OM2; thus, we explore pathways and impacts of water-mediated chemistry.

Water-mediated chemistry predicted by GEOS-Chem is linked to observations in the OM fractions in multiple regions across the CONUS and provides plausible mechanistic explanations for observations. GEOS-Chem oxidation products of isoprene produced in the aqueous mechanism (ISOAAQ) correlate significantly ($p < 0.05$) with OM2 in summer (Figure 4). This GEOS-Chem species includes carboxylic acids,[80] which are formed from the aqueous-phase chemistry of isoprene oxidation products[81,82] and observed as part of OC2 in laboratory studies.[26−28] Statistical significance is also observed for ISOAAQ with OM1 and OM4 in some regions and seasons. This is consistent with laboratory studies that demonstrate evolution of individual compounds such as oxalic acid in one or more OC thermal fraction.[17]

Decreasing summertime measured OM2 trends correlate significantly ($p < 0.05$) with decreases in measured ($R > 0.9$) and predicted ($R > 0.9$) SO_4^{2-}, ALW ($R > 0.8$), and ISOAAQ, which includes species that require the presence of water to form (Figures S9 and S10, SI).[83] The absolute and relative

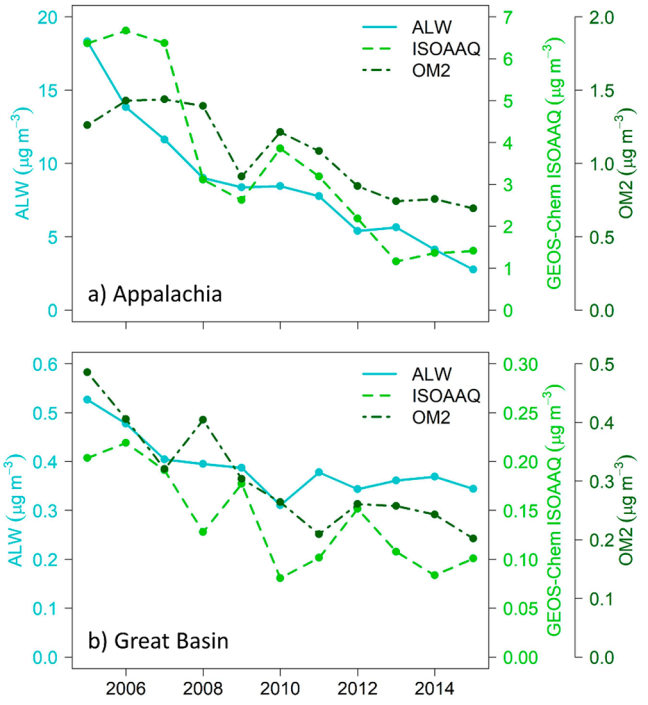

Figure 4. Decadal decreases in ALW, GEOS-Chem-predicted ISOAAQ, and OM2 for (a) Appalachia and (b) the Great Basin. Note that the *y*-axes are different between panels.

decreases are highest in the humid eastern United States during summer, where decreases in ALW are largest (Figure S5, SI). However, decreases in OM2, ALW, and ISOAAQ occur in most regions across the CONUS. For example, in the Great Basin region, representative of arid areas of the United States (Figure 4), predicted ALW mass and isoprene emissions are low,[84] yet relative decreases in OM2, ALW, and ISOAAQ are similar to observed trends in the East. This is suggestive that water-mediated processes also play a determining role in the TOC decreases outside humid locations of the eastern United States.

GEOS-Chem also predicts increases in several speciation bins, including aerosol products of light aromatics (ASOA), terpene oxidation products (TSOA), aerosols from semi-volatile organic carbon (POA), and oxidation products of primary organic gas oxidation (OPOA) (Table S1, Figure S11, SI). Many of these changes, especially OPOA (Figure S12, SI), are positively correlated with OM3, which also demonstrates increases. OPOA generally follows the same temporal pattern as OM3 in many regions, showing an increase in concentrations starting in the latter half of our analysis (Figure S13, SI). Increases in OPOA are linked to OM3 in spring, summer, and fall across the CONUS. While the TOC is reported to be decreasing, increases among positively associated independent measurements and modeled species (i.e., OM3 and OPOA) warrant further study.

Changes in OC fractions and ALW suggest changing particle properties. ALW acts as a plasticizer, and decreases in ALW lead to more viscous particles in laboratory and model studies.[85,86] It is also plausible that changes in the fractional contribution of the thermal OC fractions are indicative of altered OA viscosity.[87,88] PC decreases alongside ALW and has been linked in laboratory studies to WSOC,[16] which may suggest decreasing WSOC concentrations. As noted pre-

https://dx.doi.org/10.1021/acs.est.0c02225
Environ. Sci. Technol. 2020, 54, 10524−10532

viously, decreases in PC may be due to decreases in misapportioned LAC.[25] LAC is thought to be organic in nature[25] and could form from browning reactions in the atmosphere facilitated by ALW.[89−91] Organic speciation changes may also occur concurrent with decreasing NO_x emissions and increasing importance of autoxidation reactions.[37] These findings are consistent with a potential increase in OA viscosity and are supportive of the changing nature of organic chemical species and pathways in OA over the CONUS. This has implications for particle phase state, which affects processes including reactive uptake and particle growth[92] through changing mass transfer and bulk diffusion,[93,94] impacting the ability to quantitatively model and accurately assess aerosol impacts on climate and air quality.[95] Increased particle viscosity leads to long particle-phase diffusion time scales, which can prolong the time needed for oxidation and degradation and increase long-range transport of pollutants.

Biogenic emissions of VOCs have not changed greatly in the CONUS over the decade analyzed here and have even increased in some areas.[9,11] Decreases, most notably in inorganic anthropogenic emissions of SO_2 and NO_x, contribute to decreasing OA concentrations through a variety of mechanisms.[3,14,96] Models consistently suggest that the dominant impact is via ALW formation pathways.[13,14,79] The largest decreases in OA predicted by GEOS-Chem are strongly linked to SOA formed via aqueous pathways. Observed decreases in individual OC fractions positively associated with GEOS-Chem organic aerosol are at least partially attributable to decreases in anthropogenic emissions, most notably inorganic compounds that affect aerosol hygroscopicity to facilitate ALW uptake and SOA formation. The consistencies among independent decadal surface measurements and modeling results in humid and arid regions alike suggest that some level of chemical information is captured in routine OC fraction measurements and reproduced by models. This may offer insights into changing chemical regimes and implications for phase state, viscosity, and oxidation state of OA in the CONUS. Proper assessment of the impacts of climate, energy, and regulatory policy requires that models make accurate predictions for the right reasons. The findings here are consistent with the hypothesis that ancillary benefits occur broadly across the CONUS from federal air-quality rules aimed at ozone and acid rain through reductions in OA mass concentrations.

■ ASSOCIATED CONTENT

Supporting Information

The Supporting Information is available free of charge at https://pubs.acs.org/doi/10.1021/acs.est.0c02225.

Information on IMPROVE site and chemical climatology region locations, further analysis on OC fraction trends, and in-depth comparisons of GEOS-Chem simulations and IMPROVE measurements (Table S1 and Figures S1−S13) (PDF)

■ AUTHOR INFORMATION

Corresponding Author

Amy E. Christiansen − *Department of Chemistry, University of California, Irvine, California 92697, United States;* orcid.org/0000-0003-0114-1924; Email: amy.christiansen@mso.umt.edu

Authors

Annmarie G. Carlton − *Department of Chemistry, University of California, Irvine, California 92697, United States;* orcid.org/0000-0002-8574-1507

William C. Porter − *Department of Environmental Sciences, University of California, Riverside, California 92521, United States;* orcid.org/0000-0002-3121-8323

Complete contact information is available at: https://pubs.acs.org/10.1021/acs.est.0c02225

Author Contributions

The manuscript was written through contributions of all authors. All authors have given approval to the final version of the manuscript.

Notes

The authors declare no competing financial interest.

■ ACKNOWLEDGMENTS

This research was funded, in part, by NOAA Grant #17OAR4310103 and NSF Grant #171945. The views expressed in this paper are those of the authors and do not necessarily reflect the views or policies of the U.S. Environmental Protection Agency. The IMPROVE database can be found at http://vista.cira.colostate.edu/Improve/. IMPROVE is a collaborative association of state, tribal, and federal agencies and international partners. The US Environmental Protection Agency is the primary funding source, with contracting and research support from the National Park Service. The Air Quality Group at the University of California, Davis is the central analytical laboratory, with ion analysis provided by Research Triangle Institute and carbon analysis provided by Desert Research Institute. NCEP Reanalysis data are available from the NOAA/OAR/ESRL PSD in Boulder, Colorado, at http://www.esrl.noaa.gov/psd/. The authors gratefully acknowledge Virendra Ghate for support in retrieving NCEP Reanalysis data via the Environmental Science Division, Argonne National Laboratory, Argonne, IL, and Justin Davis for technical support. The authors also thank Athanasios Nenes and Daniel Jacob for the development and public availability of ISORROPIA and GEOS-Chem, respectively.

■ REFERENCES

(1) Zhang, Q.; Jimenez, J. L.; Canagaratna, M. R.; Allan, J. D.; Coe, H.; Ulbrich, I.; Alfarra, M. R.; Takami, A.; Middlebrook, A. M.; Sun, Y. L.; Dzepina, K.; Dunlea, E.; Docherty, K.; DeCarlo, P. F.; Salcedo, D.; Onasch, T.; Jayne, J. T.; Miyoshi, T.; Shimono, A.; Hatakeyama, S.; Takegawa, N.; Kondo, Y.; Schneider, J.; Drewnick, F.; Borrmann, S.; Weimer, S.; Demerjian, K.; Williams, P.; Bower, K.; Bahreini, R.; Cottrell, L.; Griffin, R. J.; Rautiainen, J.; Sun, J. Y.; Zhang, Y. M.; Worsnop, D. R. Ubiquity and Dominance of Oxygenated Species in Organic Aerosols in Anthropogenically-Influenced Northern Hemisphere Midlatitudes. *Geophys. Res. Lett.* **2007**, *34* (13), L13801.

(2) Ridley, D. A.; Heald, C. L.; Ridley, K. J.; Kroll, J. H. Causes and Consequences of Decreasing Atmospheric Organic Aerosol in the United States. *Proc. Natl. Acad. Sci. U. S. A.* **2018**, *115* (2), 290−295.

(3) Nguyen, T. K. V.; Capps, S. L.; Carlton, A. G. Decreasing Aerosol Water Is Consistent with OC Trends in the Southeast U.S. *Environ. Sci. Technol.* **2015**, *49* (13), 7843−7850.

(4) Attwood, A. R.; Washenfelder, R. A.; Brock, C. A.; Hu, W.; Baumann, K.; Campuzano-Jost, P.; Day, D. A.; Edgerton, E. S.; Murphy, D. M.; Palm, B. B.; McComiskey, A.; Wagner, N. L.; de Sá, S. S.; Ortega, A.; Martin, S. T.; Jimenez, J. L.; Brown, S. S. Trends in Sulfate and Organic Aerosol Mass in the Southeast U.S.: Impact on

Aerosol Optical Depth and Radiative Forcing: Aerosol Mass and Optical Depth in SE US. *Geophys. Res. Lett.* **2014**, *41* (21), 7701−7709.
(5) Blanchard, C. L.; Tanenbaum, S.; Hidy, G. M. Source Attribution of Air Pollutant Concentrations and Trends in the Southeastern Aerosol Research and Characterization (SEARCH) Network. *Environ. Sci. Technol.* **2013**, *47* (23), 13536−13545.
(6) Malm, W. C.; Schichtel, B. A.; Hand, J. L.; Collett, J. L. Concurrent Temporal and Spatial Trends in Sulfate and Organic Mass Concentrations Measured in the IMPROVE Monitoring Program: Trends in Sulfate and Organic Mass. *J. Geophys. Res. Atmospheres* **2017**, *122* (19), 10462−10476.
(7) Bench, G.; Fallon, S.; Schichtel, B.; Malm, W.; McDade, C. Relative Contributions of Fossil and Contemporary Carbon Sources to $PM_{2.5}$ Aerosols at Nine Interagency Monitoring for Protection of Visual Environments (IMPROVE) Network Sites. *J. Geophys. Res. Atmospheres* **2007**, *112* (D10), D10205.
(8) Schichtel, B. A.; Malm, W. C.; Bench, G.; Fallon, S.; McDade, C. E.; Chow, J. C.; Watson, J. G. Fossil and Contemporary Fine Particulate Carbon Fractions at 12 Rural and Urban Sites in the United States. *J. Geophys. Res.* **2008**, *113* (D2), D02311.
(9) Heald, C. L.; Henze, D. K.; Horowitz, L. W.; Feddema, J.; Lamarque, J.-F.; Guenther, A.; Hess, P. G.; Vitt, F.; Seinfeld, J. H.; Goldstein, A. H.; Fung, I. Predicted Change in Global Secondary Organic Aerosol Concentrations in Response to Future Climate, Emissions, and Land Use Change. *J. Geophys. Res. Atmospheres* **2008**, *113* (D5), D05211.
(10) Heal, M. R. The Application of Carbon-14 Analyses to the Source Apportionment of Atmospheric Carbonaceous Particulate Matter: A Review. *Anal. Bioanal. Chem.* **2014**, *406* (1), 81−98.
(11) Spracklen, D. V.; Mickley, L. J.; Logan, J. A.; Hudman, R. C.; Yevich, R.; Flannigan, M. D.; Westerling, A. L. Impacts of Climate Change from 2000 to 2050 on Wildfire Activity and Carbonaceous Aerosol Concentrations in the Western United States. *J. Geophys. Res.* **2009**, *114* (D20), D20301.
(12) Westerling, A. L. Increasing Western US Forest Wildfire Activity: Sensitivity to Changes in the Timing of Spring. *Philos. Trans. R. Soc., B* **2016**, *371* (1696), 20150178.
(13) Carlton, A. G.; Pye, H. O. T.; Baker, K. R.; Hennigan, C. J. Additional Benefits of Federal Air-Quality Rules: Model Estimates of Controllable Biogenic Secondary Organic Aerosol. *Environ. Sci. Technol.* **2018**, *52* (16), 9254−9265.
(14) Marais, E. A.; Jacob, D. J.; Turner, J. R.; Mickley, L. J. Evidence of 1991−2013 Decrease of Biogenic Secondary Organic Aerosol in Response to SO_2 Emission Controls. *Environ. Res. Lett.* **2017**, *12* (5), 054018.
(15) Marais, E. A.; Jacob, D. J.; Jimenez, J. L.; Campuzano-Jost, P.; Day, D. A.; Hu, W.; Krechmer, J.; Zhu, L.; Kim, P. S.; Miller, C. C.; Fisher, J. A.; Travis, K.; Yu, K.; Hanisco, T. F.; Wolfe, G. M.; Arkinson, H. L.; Pye, H. O. T.; Froyd, K. D.; Liao, J.; McNeill, V. F. Aqueous-Phase Mechanism for Secondary Organic Aerosol Formation from Isoprene: Application to the Southeast United States and Co-Benefit of SO_2 Emission Controls. *Atmos. Chem. Phys.* **2016**, *16* (3), 1603−1618.
(16) Khan, B.; Hays, M. D.; Geron, C.; Jetter, J. Differences in the OC/EC Ratios That Characterize Ambient and Source Aerosols Due to Thermal-Optical Analysis. *Aerosol Sci. Technol.* **2012**, *46* (2), 127−137.
(17) Meier, S. M.; Schwab, J. J. *Beyond OC--A Method to Extract and Interpret Additional Aerosol Organic Carbon Fractions from Thermal Optical Analysis of Filter-Based and Continuous Data*; New York State Energy Research and Development Authority, 2011.
(18) Chow, J. C.; Watson, J. G.; Pritchett, L. C.; Pierson, W. R.; Frazier, C. A.; Purcell, R. G. The Dri Thermal/Optical Reflectance Carbon Analysis System: Description, Evaluation and Applications in U.S. Air Quality Studies. *Atmos. Environ., Part A* **1993**, *27* (8), 1185−1201.
(19) Rau, J. A. *Residential Wood Combustion Aerosol Characterization as a Function of Size and Source Apportionment Using Chemical Mass Balance Modeling*; Oregon Graduate Center: Beaverton, OR, 1986.
(20) Chow, J. C.; Watson, J. G.; Chen, L.-W. A.; Chang, M. C. O.; Robinson, N. F.; Trimble, D.; Kohl, S. The IMPROVE_A Temperature Protocol for Thermal/Optical Carbon Analysis: Maintaining Consistency with a Long-Term Database. *J. Air Waste Manage. Assoc.* **2007**, *57* (9), 1014−1023.
(21) Chow, J.; Watson, J. G.; Chen, L.-W. A.; Chang, M.-C. O.; Paredes-Miranda, G. *Comparison of the DRI/OGC and Model 2001 Thermal/Optical Carbon Analyzers*; Desert Research Institute, 2005.
(22) Wang, Y.; Chung, A.; Paulson, S. E. The Effect of Metal Salts on Quantification of Elemental and Organic Carbon in Diesel Exhaust Particles Using Thermal-Optical Evolved Gas Analysis. *Atmos. Chem. Phys.* **2010**, *10* (23), 11447−11457.
(23) Baumgardner, D.; Popovicheva, O.; Allan, J.; Bernardoni, V.; Cao, J.; Cavalli, F.; Cozic, J.; Diapouli, E.; Eleftheriadis, K.; Genberg, P. J.; Gonzalez, C.; Gysel, M.; John, A.; Kirchstetter, T. W.; Kuhlbusch, T. A. J.; Laborde, M.; Lack, D.; Müller, T.; Niessner, R.; Petzold, A.; Piazzalunga, A.; Putaud, J. P.; Schwarz, J.; Sheridan, P.; Subramanian, R.; Swietlicki, E.; Valli, G.; Vecchi, R.; Viana, M. Soot Reference Materials for Instrument Calibration and Intercomparisons: A Workshop Summary with Recommendations. *Atmos. Meas. Tech.* **2012**, *5* (8), 1869−1887.
(24) Chow, J. C.; Watson, J. G. $PM_{2.5}$ Carbonate Concentrations at Regionally Representative Interagency Monitoring of Protected Visual Environment Sites. *J. Geophys. Res. Atmospheres* **2002**, *107* (D21), ICC 6-1.
(25) Malm, W. C.; Schichtel, B. A.; Hand, J. L.; Prenni, A. J. Implications of Organic Mass to Carbon Ratios Increasing Over Time in the Rural United States. *J. Geophys. Res.: Atmos.* **2020**, *125* (5), e2019JD031480.
(26) Chow, J. C.; Watson, J. G.; Kuhns, H.; Etyemezian, V.; Lowenthal, D. H.; Crow, D.; Kohl, S. D.; Engelbrecht, J. P.; Green, M. C. Source Profiles for Industrial, Mobile, and Area Sources in the Big Bend Regional Aerosol Visibility and Observational Study. *Chemosphere* **2004**, *54* (2), 185−208.
(27) Cao, J. J.; Wu, F.; Chow, J. C.; Lee, S. C.; Li, Y.; Chen, S. W.; An, Z. S.; Fung, K. K.; Watson, J. G.; Zhu, C. S.; Liu, S. X. Characterization and Source Apportionment of Atmospheric Organic and Elemental Carbon during Fall and Winter of 2003 in Xi'an, China. *Atmos. Chem. Phys.* **2005**, *5* (11), 3127−3137.
(28) Aswini, A. R.; Hegde, P.; Nair, P. R.; Aryasree, S. Seasonal Changes in Carbonaceous Aerosols over a Tropical Coastal Location in Response to Meteorological Processes. *Sci. Total Environ.* **2019**, *656*, 1261−1279.
(29) Lim, S.; Lee, M.; Lee, G.; Kim, S.; Yoon, S.; Kang, K. Ionic and Carbonaceous Compositions of PM_{10}, $PM_{2.5}$ and $PM_{1.0}$ at Gosan ABC Superstation and Their Ratios as Source Signature. *Atmos. Chem. Phys.* **2012**, *12* (4), 2007−2024.
(30) Miyazaki, Y.; Kondo, Y.; Han, S.; Koike, M.; Kodama, D.; Komazaki, Y.; Tanimoto, H.; Matsueda, H. Chemical Characteristics of Water-Soluble Organic Carbon in the Asian Outflow. *J. Geophys. Res.* **2007**, *112* (D22), D22S30.
(31) Dillner, A. M.; Takahama, S. Predicting Ambient Aerosol Thermal-Optical Reflectance (TOR) Measurements from Infrared Spectra: Organic Carbon. *Atmos. Meas. Tech.* **2015**, *8* (3), 1097−1109.
(32) Kamruzzaman, M.; Takahama, S.; Dillner, A. M. Quantification of Amine Functional Groups and Their Influence on OM/OC in the IMPROVE Network. *Atmos. Environ.* **2018**, *172*, 124−132.
(33) Weakley, A. T.; Takahama, S.; Dillner, A. M. Ambient Aerosol Composition by Infrared Spectroscopy and Partial Least-Squares in the Chemical Speciation Network: Organic Carbon with Functional Group Identification. *Aerosol Sci. Technol.* **2016**, *50* (10), 1096−1114.
(34) Rothfuss, N. E.; Petters, M. D. Influence of Functional Groups on the Viscosity of Organic Aerosol. *Environ. Sci. Technol.* **2017**, *51* (1), 271−279.

https://dx.doi.org/10.1021/acs.est.0c02225
Environ. Sci. Technol. 2020, 54, 10524−10532

(35) Simon, H.; Reff, A.; Wells, B.; Xing, J.; Frank, N. Ozone Trends Across the United States over a Period of Decreasing NO_x and VOC Emissions. *Environ. Sci. Technol.* **2015**, *49* (1), 186−195.
(36) Seinfeld, J. H.; Pandis, S. N. *Atmospheric Chemistry and Physics: From Air Pollution to Climate Change*; Wiley: New York, 1998.
(37) Praske, E.; Otkjær, R. V.; Crounse, J. D.; Hethcox, J. C.; Stoltz, B. M.; Kjaergaard, H. G.; Wennberg, P. O. Atmospheric Autoxidation Is Increasingly Important in Urban and Suburban North America. *Proc. Natl. Acad. Sci. U. S. A.* **2018**, *115* (1), 64−69.
(38) Hand, J. L.; Prenni, A. J.; Schichtel, B. A.; Malm, W. C.; Chow, J. C. Trends in Remote $PM_{2.5}$ Residual Mass across the United States: Implications for Aerosol Mass Reconstruction in the IMPROVE Network. *Atmos. Environ.* **2019**, *203*, 141−152.
(39) Chow, J. C.; Watson, J. G.; Green, M. C.; Wang, X.; Chen, L.-W. A.; Trimble, D. L.; Cropper, P. M.; Kohl, S. D.; Gronstal, S. B. Separation of Brown Carbon from Black Carbon for IMPROVE and Chemical Speciation Network $PM_{2.5}$ Samples. *J. Air Waste Manage. Assoc.* **2018**, *68* (5), 494−510.
(40) Hyslop, N.; White, W. An Evaluation of Interagency Monitoring of Protected Visual Environments (IMPROVE) Collocated Precision and Uncertainty Estimates. *Atmos. Environ.* **2008**, *42* (11), 2691−2705.
(41) Dillner, A. M.; Phuah, C. H.; Turner, J. R. Effects of Post-Sampling Conditions on Ambient Carbon Aerosol Filter Measurements. *Atmos. Environ.* **2009**, *43* (37), 5937−5943.
(42) Malm, W. C.; Schichtel, B. A.; Pitchford, M. L. Uncertainties in $PM_{2.5}$ Gravimetric and Speciation Measurements and What We Can Learn from Them. *J. Air Waste Manage. Assoc.* **2011**, *61* (11), 1131−1149.
(43) Chow, J. C.; Lowenthal, D. H.; Chen, L.-W. A.; Wang, X.; Watson, J. G. Mass Reconstruction Methods for $PM_{2.5}$: A Review. *Air Qual., Atmos. Health* **2015**, *8* (3), 243−263.
(44) Boparai, P.; Lee, J.; Bond, T. C. Revisiting Thermal-Optical Analyses of Carbonaceous Aerosol Using a Physical Model. *Aerosol Sci. Technol.* **2008**, *42* (11), 930−948.
(45) Subramanian, R.; Khlystov, A. Y.; Robinson, A. L. Effect of Peak Inert-Mode Temperature on Elemental Carbon Measured Using Thermal-Optical Analysis. *Aerosol Sci. Technol.* **2006**, *40* (10), 763−780.
(46) Simon, H.; Bhave, P. V.; Swall, J. L.; Frank, N. H.; Malm, W. C. Determining the Spatial and Seasonal Variability in OM/OC Ratios across the US Using Multiple Regression. *Atmos. Chem. Phys.* **2011**, *11* (6), 2933−2949.
(47) Philip, S.; Martin, R. V.; Pierce, J. R.; Jimenez, J. L.; Zhang, Q.; Canagaratna, M. R.; Spracklen, D. V.; Nowlan, C. R.; Lamsal, L. N.; Cooper, M. J.; Krotkov, N. A. Spatially and Seasonally Resolved Estimate of the Ratio of Organic Mass to Organic Carbon. *Atmos. Environ.* **2014**, *87*, 34−40.
(48) El-Zanan, H. S.; Lowenthal, D. H.; Zielinska, B.; Chow, J. C.; Kumar, N. Determination of the Organic Aerosol Mass to Organic Carbon Ratio in IMPROVE Samples. *Chemosphere* **2005**, *60* (4), 485−496.
(49) Aiken, A. C.; DeCarlo, P. F.; Kroll, J. H.; Worsnop, D. R.; Huffman, J. A.; Docherty, K. S.; Ulbrich, I. M.; Mohr, C.; Kimmel, J. R.; Sueper, D.; Sun, Y.; Zhang, Q.; Trimborn, A.; Northway, M.; Ziemann, P. J.; Canagaratna, M. R.; Onasch, T. B.; Alfarra, M. R.; Prevot, A. S. H.; Dommen, J.; Duplissy, J.; Metzger, A.; Baltensperger, U.; Jimenez, J. L. O/C and OM/OC Ratios of Primary, Secondary, and Ambient Organic Aerosols with High-Resolution Time-of-Flight Aerosol Mass Spectrometry. *Environ. Sci. Technol.* **2008**, *42* (12), 4478−4485.
(50) Ruthenburg, T. C.; Perlin, P. C.; Liu, V.; McDade, C. E.; Dillner, A. M. Determination of Organic Matter and Organic Matter to Organic Carbon Ratios by Infrared Spectroscopy with Application to Selected Sites in the IMPROVE Network. *Atmos. Environ.* **2014**, *86*, 47−57.
(51) Air Quality Research Center. *Interagency Monitoring of Protected Visual Environments (IMPROVE) Semiannual Quality Assurance Report: January 1, 2018 through December 31, 2018*; Air Quality Research Center, University of California, Davis: Davis, CA, November 15, 2019.
(52) Lowenthal, D. H.; Kumar, N. $PM_{2.5}$ Mass and Light Extinction Reconstruction in IMPROVE. *J. Air Waste Manage. Assoc.* **2003**, *53* (9), 1109−1120.
(53) Bae, M.; Demerjian, K.; Schwab, J. Seasonal Estimation of Organic Mass to Organic Carbon in PM2.5 at Rural and Urban Locations in New York State. *Atmos. Environ.* **2006**, *40* (39), 7467−7479.
(54) Fountoukis, C.; Nenes, A. ISORROPIA II: A Computationally Efficient Thermodynamic Equilibrium Model for K^+-Ca^{2+}-Mg^{2+}-NH_4^+-Na^+-SO_4^{2-}-NO_3^--Cl^--H_2O Aerosols. *Atmos. Chem. Phys.* **2007**, *7* (17), 4639−4659.
(55) Nguyen, T. K. V.; Ghate, V. P.; Carlton, A. G. Reconciling Satellite Aerosol Optical Thickness and Surface Fine Particle Mass through Aerosol Liquid Water. *Geophys. Res. Lett.* **2016**, *43* (22), 11903−11912.
(56) Metzger, S.; Abdelkader, M.; Steil, B.; Klingmüller, K. Aerosol Water Parameterization: Long-Term Evaluation and Importance for Climate Studies. *Atmos. Chem. Phys.* **2018**, *18*, 16747−16774.
(57) Jathar, S. H.; Mahmud, A.; Barsanti, K. C.; Asher, W. E.; Pankow, J. F.; Kleeman, M. J. Water Uptake by Organic Aerosol and Its Influence on Gas/Particle Partitioning of Secondary Organic Aerosol in the United States. *Atmos. Environ.* **2016**, *129*, 142−154.
(58) Christiansen, A. E.; Ghate, V. P.; Carlton, A. G. Aerosol Optical Thickness: Organic Composition, Associated Particle Water, and Aloft Extinction. *ACS Earth Space Chem.* **2019**, *3* (3), 403−412.
(59) Christiansen, A. E.; Carlton, A. G.; Henderson, B. H. Differences in Fine Particle Chemical Composition on Clear and Cloudy Days. *Atmos. Chem. Phys. Discuss.* **2020**, DOI: 10.5194/acp-2020-184.
(60) Gelaro, R.; McCarty, W.; Suárez, M. J.; Todling, R.; Molod, A.; Takacs, L.; Randles, C. A.; Darmenov, A.; Bosilovich, M. G.; Reichle, R.; Wargan, K.; Coy, L.; Cullather, R.; Draper, C.; Akella, S.; Buchard, V.; Conaty, A.; da Silva, A. M.; Gu, W.; Kim, G.-K.; Koster, R.; Lucchesi, R.; Merkova, D.; Nielsen, J. E.; Partyka, G.; Pawson, S.; Putman, W.; Rienecker, M.; Schubert, S. D.; Sienkiewicz, M.; Zhao, B. The Modern-Era Retrospective Analysis for Research and Applications, Version 2 (MERRA-2). *J. Clim.* **2017**, *30* (14), 5419−5454.
(61) Travis, K. R.; Jacob, D. J.; Fisher, J. A.; Kim, P. S.; Marais, E. A.; Zhu, L.; Yu, K.; Miller, C. C.; Yantosca, R. M.; Sulprizio, M. P.; Thompson, A. M.; Wennberg, P. O.; Crounse, J. D.; St. Clair, J. M.; Cohen, R. C.; Laughner, J. L.; Dibb, J. E.; Hall, S. R.; Ullmann, K.; Wolfe, G. M.; Pollack, I. B.; Peischl, J.; Neuman, J. A.; Zhou, X. Why Do Models Overestimate Surface Ozone in the Southeast United States? *Atmos. Chem. Phys.* **2016**, *16* (21), 13561−13577.
(62) Guenther, A. B.; Jiang, X.; Heald, C. L.; Sakulyanontvittaya, T.; Duhl, T.; Emmons, L. K.; Wang, X. The Model of Emissions of Gases and Aerosols from Nature Version 2.1 (MEGAN2.1): An Extended and Updated Framework for Modeling Biogenic Emissions. *Geosci. Model Dev.* **2012**, *5* (6), 1471−1492.
(63) Millet, D. B.; Guenther, A.; Siegel, D. A.; Nelson, N. B.; Singh, H. B.; de Gouw, J. A.; Warneke, C.; Williams, J.; Eerdekens, G.; Sinha, V.; Karl, T.; Flocke, F.; Apel, E.; Riemer, D. D.; Palmer, P. I.; Barkley, M. Global Atmospheric Budget of Acetaldehyde: 3-D Model Analysis and Constraints from in-Situ and Satellite Observations. *Atmos. Chem. Phys.* **2010**, *10* (7), 3405−3425.
(64) Tai, A. P. K.; Mickley, L. J.; Heald, C. L.; Wu, S. Effect of CO_2 Inhibition on Biogenic Isoprene Emission: Implications for Air Quality under 2000 to 2050 Changes in Climate, Vegetation, and Land Use. *Geophys. Res. Lett.* **2013**, *40* (13), 3479−3483.
(65) Yuan, H.; Dai, Y.; Xiao, Z.; Ji, D.; Shangguan, W. Reprocessing the MODIS Leaf Area Index Products for Land Surface and Climate Modelling. *Remote Sens. Environ.* **2011**, *115* (5), 1171−1187.
(66) Giglio, L.; Randerson, J. T.; van der Werf, G. R. Analysis of Daily, Monthly, and Annual Burned Area Using the Fourth-Generation Global Fire Emissions Database (GFED4). *J. Geophys. Res.: Biogeosci.* **2013**, *118* (1), 317−328.

(67) van der Werf, G. R.; Randerson, J. T.; Giglio, L.; Collatz, G. J.; Mu, M.; Kasibhatla, P. S.; Morton, D. C.; DeFries, R. S.; Jin, Y.; van Leeuwen, T. T. Global Fire Emissions and the Contribution of Deforestation, Savanna, Forest, Agricultural, and Peat Fires (1997−2009). *Atmos. Chem. Phys.* **2010**, *10* (23), 11707−11735.
(68) Pye, H. O. T.; Chan, A. W. H.; Barkley, M. P.; Seinfeld, J. H. Global Modeling of Organic Aerosol: The Importance of Reactive Nitrogen (NO_x and NO_3). *Atmos. Chem. Phys.* **2010**, *10* (22), 11261−11276.
(69) Fisher, J. A.; Jacob, D. J.; Travis, K. R.; Kim, P. S.; Marais, E. A.; Chan Miller, C.; Yu, K.; Zhu, L.; Yantosca, R. M.; Sulprizio, M. P.; Mao, J.; Wennberg, P. O.; Crounse, J. D.; Teng, A. P.; Nguyen, T. B.; St. Clair, J. M.; Cohen, R. C.; Romer, P.; Nault, B. A.; Wooldridge, P. J.; Jimenez, J. L.; Campuzano-Jost, P.; Day, D. A.; Hu, W.; Shepson, P. B.; Xiong, F.; Blake, D. R.; Goldstein, A. H.; Misztal, P. K.; Hanisco, T. F.; Wolfe, G. M.; Ryerson, T. B.; Wisthaler, A.; Mikoviny, T. Organic Nitrate Chemistry and Its Implications for Nitrogen Budgets in an Isoprene- and Monoterpene-Rich Atmosphere: Constraints from Aircraft (SEAC^{4}RS) and Ground-Based (SOAS) Observations in the Southeast US. *Atmos. Chem. Phys.* **2016**, *16* (9), 5969−5991.
(70) Theil, H. A Rank-Invariant Method of Linear and Polynomial Regression Analysis I, II and III. *Proc. R. Neth. Acad. Sci.* **1950**, *53*, 386−392.
(71) Sen, P. K. Estimates of the Regression Coefficient Based on Kendall's Tau. *J. Am. Stat. Assoc.* **1968**, *63* (324), 1379−1389.
(72) R Core Team. *R: A Language and Environment for Statistical Computing*; R Foundation for Statistical Computing: Vienna, Austria, 2013.
(73) Mann, H. B. Nonparametric Tests Against Trend. *Econometrica* **1945**, *13* (3), 245−259.
(74) Kendall, M. G. *Rank Correlation Methods*; Charles Griffin: London, 1975.
(75) Dat, N.-D.; Chang, M. B. Review on Characteristics of PAHs in Atmosphere, Anthropogenic Sources and Control Technologies. *Sci. Total Environ.* **2017**, *609*, 682−693.
(76) Abdel-Shafy, H. I.; Mansour, M. S. M. A Review on Polycyclic Aromatic Hydrocarbons: Source, Environmental Impact, Effect on Human Health and Remediation. *Egypt. J. Pet.* **2016**, *25* (1), 107−123.
(77) Ruehl, C. R.; Ham, W. A.; Kleeman, M. J. Temperature-Induced Volatility of Molecular Markers in Ambient Airborne Particulate Matter. *Atmos. Chem. Phys.* **2011**, *11* (1), 67−76.
(78) Ferrero, L.; Sangiorgi, G.; Perrone, M.; Rizzi, C.; Cataldi, M.; Markuszewski, P.; Pakszys, P.; Makuch, P.; Petelski, T.; Becagli, S.; Traversi, R.; Bolzacchini, E.; Zielinski, T. Chemical Composition of Aerosol over the Arctic Ocean from Summer ARctic EXpedition (AREX) 2011−2012 Cruises: Ions, Amines, Elemental Carbon, Organic Matter, Polycyclic Aromatic Hydrocarbons, n-Alkanes, Metals, and Rare Earth Elements. *Atmosphere* **2019**, *10* (2), 54.
(79) Carlton, A. G.; Turpin, B. J. Particle Partitioning Potential of Organic Compounds Is Highest in the Eastern US and Driven by Anthropogenic Water. *Atmos. Chem. Phys.* **2013**, *13* (20), 10203−10214.
(80) Nguyen, T. B.; Bateman, A. P.; Bones, D. L.; Nizkorodov, S. A.; Laskin, J.; Laskin, A. High-Resolution Mass Spectrometry Analysis of Secondary Organic Aerosol Generated by Ozonolysis of Isoprene. *Atmos. Environ.* **2010**, *44* (8), 1032−1042.
(81) Tan, Y.; Carlton, A. G.; Seitzinger, S. P.; Turpin, B. J. SOA from Methylglyoxal in Clouds and Wet Aerosols: Measurement and Prediction of Key Products. *Atmos. Environ.* **2010**, *44* (39), 5218−5226.
(82) Carlton, A. G.; Turpin, B. J.; Lim, H.-J.; Altieri, K. E.; Seitzinger, S. Link between Isoprene and Secondary Organic Aerosol (SOA): Pyruvic Acid Oxidation Yields Low Volatility Organic Acids in Clouds. *Geophys. Res. Lett.* **2006**, *33* (6), L06822.
(83) Nguyen, T. B.; Coggon, M. M.; Bates, K. H.; Zhang, X.; Schwantes, R. H.; Schilling, K. A.; Loza, C. L.; Flagan, R. C.; Wennberg, P. O.; Seinfeld, J. H. Organic Aerosol Formation from the Reactive Uptake of Isoprene Epoxydiols (IEPOX) onto Non-Acidified Inorganic Seeds. *Atmos. Chem. Phys.* **2014**, *14* (7), 3497−3510.
(84) Wang, P.; Schade, G.; Estes, M.; Ying, Q. Improved MEGAN Predictions of Biogenic Isoprene in the Contiguous United States. *Atmos. Environ.* **2017**, *148*, 337−351.
(85) Reid, J. P.; Bertram, A. K.; Topping, D. O.; Laskin, A.; Martin, S. T.; Petters, M. D.; Pope, F. D.; Rovelli, G. The Viscosity of Atmospherically Relevant Organic Particles. *Nat. Commun.* **2018**, *9* (1), 956.
(86) O'Meara, S.; Topping, D. O.; McFiggans, G. The Rate of Equilibration of Viscous Aerosol Particles. *Atmos. Chem. Phys.* **2016**, *16* (8), 5299−5313.
(87) Champion, W. M.; Rothfuss, N. E.; Petters, M. D.; Grieshop, A. P. Volatility and Viscosity Are Correlated in Terpene Secondary Organic Aerosol Formed in a Flow Reactor. *Environ. Sci. Technol. Lett.* **2019**, *6*, 513−519.
(88) Yli-Juuti, T.; Pajunoja, A.; Tikkanen, O.; Buchholz, A.; Faiola, C.; Väisänen, O.; Hao, L.; Kari, E.; Peräkylä, O.; Garmash, O.; Shiraiwa, M.; Ehn, M.; Lehtinen, K.; Virtanen, A. Factors Controlling the Evaporation of Secondary Organic Aerosol from A-pinene Ozonolysis. *Geophys. Res. Lett.* **2017**, *44* (5), 2562−2570.
(89) Chang, J. L.; Thompson, J. E. Characterization of Colored Products Formed during Irradiation of Aqueous Solutions Containing H_2O_2 and Phenolic Compounds. *Atmos. Environ.* **2010**, *44* (4), 541−551.
(90) Sareen, N.; Schwier, A. N.; Shapiro, E. L.; Mitroo, D.; McNeill, V. F. Secondary Organic Material Formed by Methylglyoxal in Aqueous Aerosol Mimics. *Atmos. Chem. Phys.* **2010**, *10* (3), 997−1016.
(91) De Haan, D. O.; Corrigan, A. L.; Smith, K. W.; Stroik, D. R.; Turley, J. J.; Lee, F. E.; Tolbert, M. A.; Jimenez, J. L.; Cordova, K. E.; Ferrell, G. R. Secondary Organic Aerosol-Forming Reactions of Glyoxal with Amino Acids. *Environ. Sci. Technol.* **2009**, *43* (8), 2818−2824.
(92) Li, Y.; Shiraiwa, M. Timescales of Secondary Organic Aerosols to Reach Equilibrium at Various Temperatures and Relative Humidities. *Atmos. Chem. Phys.* **2019**, *19* (9), 5959−5971.
(93) Berkemeier, T.; Steimer, S. S.; Krieger, U. K.; Peter, T.; Pöschl, U.; Ammann, M.; Shiraiwa, M. Ozone Uptake on Glassy, Semi-Solid and Liquid Organic Matter and the Role of Reactive Oxygen Intermediates in Atmospheric Aerosol Chemistry. *Phys. Chem. Chem. Phys.* **2016**, *18* (18), 12662−12674.
(94) Marshall, F. H.; Miles, R. E. H.; Song, Y.-C.; Ohm, P. B.; Power, R. M.; Reid, J. P.; Dutcher, C. S. Diffusion and Reactivity in Ultraviscous Aerosol and the Correlation with Particle Viscosity. *Chem. Sci.* **2016**, *7* (2), 1298−1308.
(95) Shiraiwa, M.; Li, Y.; Tsimpidi, A. P.; Karydis, V. A.; Berkemeier, T.; Pandis, S. N.; Lelieveld, J.; Koop, T.; Pöschl, U. Global Distribution of Particle Phase State in Atmospheric Secondary Organic Aerosols. *Nat. Commun.* **2017**, *8* (1), 15002.
(96) Lane, T. E.; Donahue, N. M.; Pandis, S. N. Effect of NO_x on Secondary Organic Aerosol Concentrations. *Environ. Sci. Technol.* **2008**, *42* (16), 6022−6027.

https://dx.doi.org/10.1021/acs.est.0c02225
Environ. Sci. Technol. 2020, 54, 10524−10532